

Modelling atmospheric chemistry and long-range transport of emerging Asian pollutants

¹Kuo-Ying Wang and ²Dudley E. Shallcross

¹Department of Atmospheric Sciences, National Central University, Chung-Li, Taiwan

²School of Chemistry, Cantock's Close, University of Bristol, Bristol BS8 1TS, UK

Abstract

Modeling is a very important tool for scientific processes, requiring long-term dedication, desire, and continuous reflection. In this work, we discuss several aspects of modeling, and the reasons for doing it. We discuss two major modeling systems that have been built by us over the last 10 years. It is a long and arduous process but the reward of understanding can be enormous, as demonstrated in the examples shown in this work. We found that long-range transport of emerging Asian pollutants can be interpreted using a Lagrangian framework for wind analysis. More detailed processes still need to be modeled but an accurate representation of the wind structure is the most important thing above all others. Our long-term chemistry integrations reveal the capability of the IMS model in simulating tropospheric chemistry on a climate scale. These long-term integrations also show ways for further model development. Modeling is a quantitative process, and the understanding can be sustained only when theories are vigorously tested in the models and compared with high quality measurements. We should also not overlook the importance of data visualization techniques. Humans feel more confident when they see things. Hence, modeling is an incredible journey, combining data collection, theoretical formulation, detailed computer coding and harnessing computer power. The best is yet to come.

1. What is Modelling?

The Earth's climate is a classic example of a highly complex, coupled system where scientific progress depends on models that can synthesise observations, theory, and experimental results to investigate how the Earth system works and how it may be affected by human activities (CCSP, 2001). Figure 1 is a schematic diagram showing a real world and the processes for making models of a real world (Jackson, 1991). The real world that we live in in our daily life is a very complicated system. In order to comprehend the inner workings of the machinery of the real world, we build models and test models against the real world observations. In doing so, we gain an understanding of the real world. We should bear in mind that the most important goal for modelling is to progress our understanding, followed by modelling for societal benefit (Wilderspin, 2002). Since the real world is already a very complicated system, it makes no sense at all to build another very complicated world produced by models that are well beyond the grasp of our comprehension and that cannot be validated by comparison with observations. Given the wide ranges of models now freely available in the public domain, we should be aware of the increasing gap between modelling and understanding (e.g., Held, 2005). We should also clearly make

Fig. 1.3

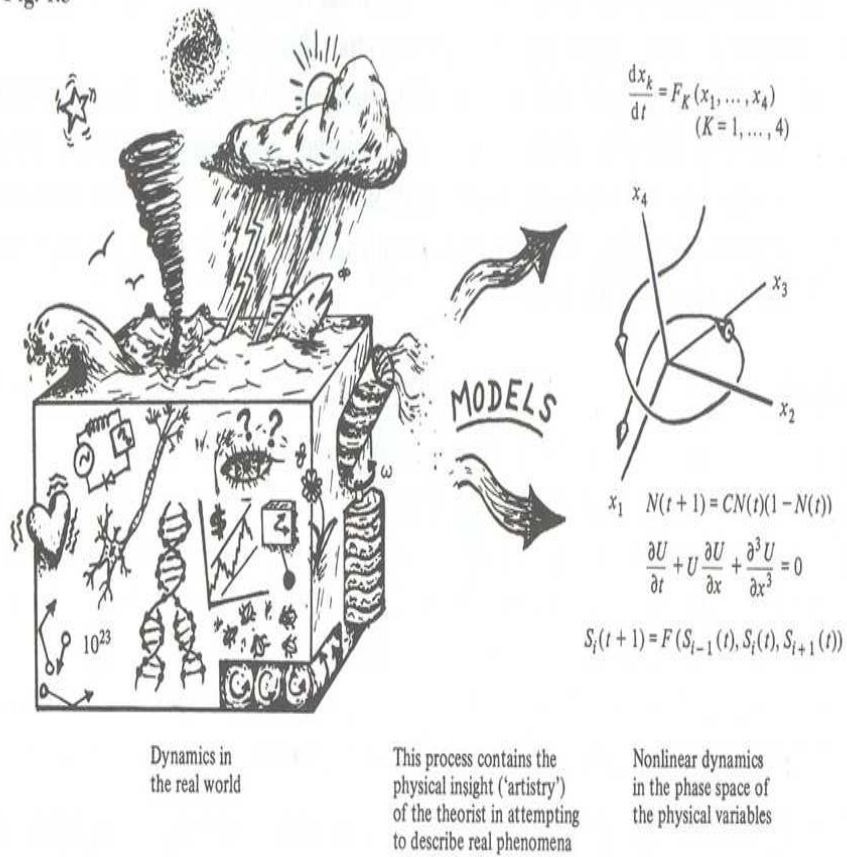


Figure 1: A schematic diagram showing the complex real world (left panel), and the processes for understanding real-world events through modeling processes. This figure is taken from Jackson (1991).

distinctions between models, modelling, simulations, and understanding. It is also necessary to tell the difference between forecast and prediction (Cyranoski, 2004). The benefit of modelling will be lost if not understanding is obtained at the end. If there is no advancement to our understanding, then our capacity to make predictions about the future states of our atmosphere remains very limited.

1. Why Atmospheric Chemistry Modelling?

2.1. A Chemistry-Climate Perspective

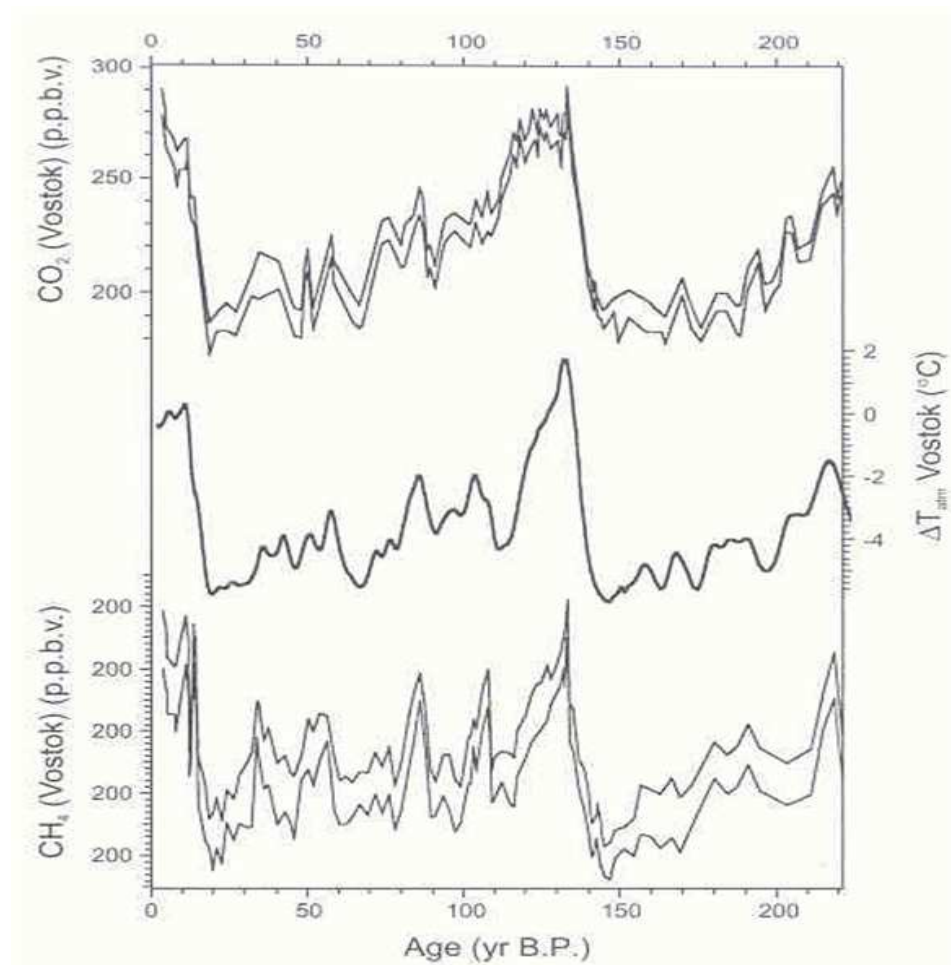


Figure 2: Variations of CO_2 , CH_4 and atmospheric temperatures over Vostok for the past 220 thousand years. This figure is taken from Jouzel et al. (1993).

From a chemistry-climate perspective, there exists a strong correlation between concentrations of greenhouse gases and variations in surface temperature. Figure 2 shows variations of carbon dioxide, methane and surface temperature

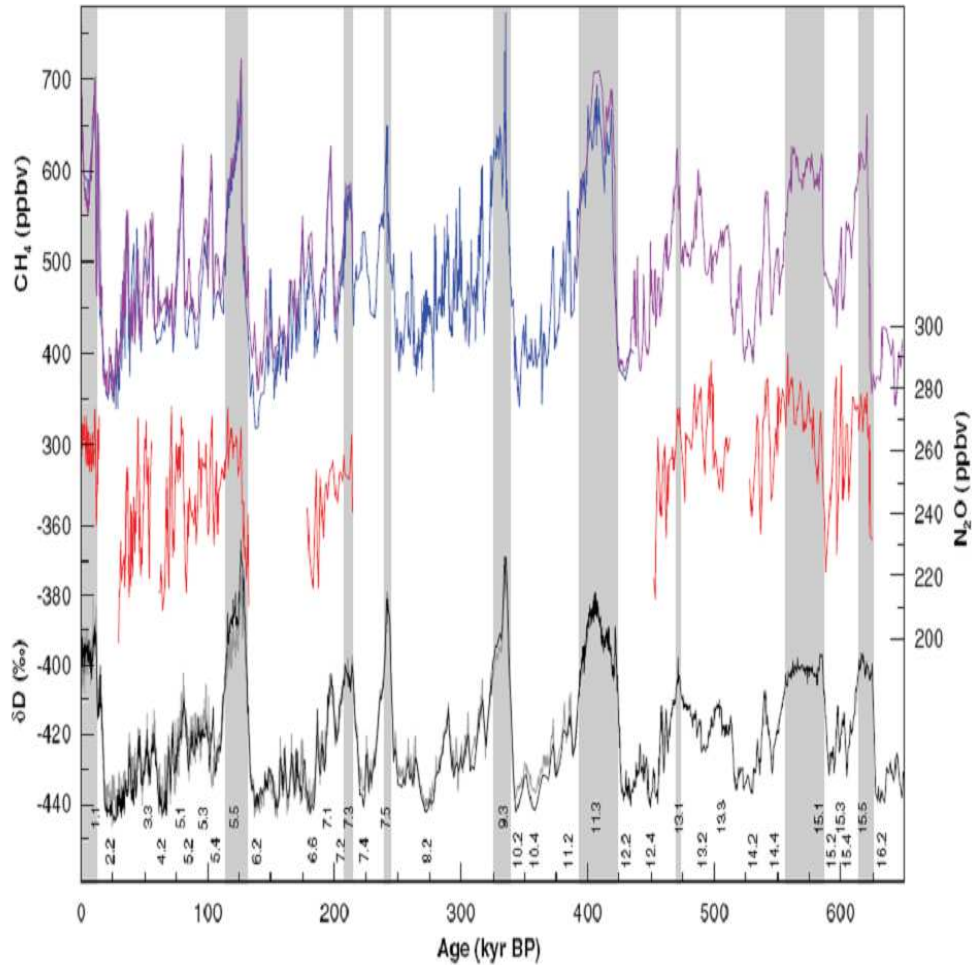


Figure 3: Variations of CH_4 , N_2O and δD records for the past 650 thousand years from Antarctic ice cores. This figure is taken from Spahni et al. (2005).

for the past 220 thousand years. The period of peaks (inter-glacials) and troughs (glacials) in temperatures correlate very well with peaks and troughs in the atmospheric levels of methane and carbon dioxide. Recent studies have pushed the reconstruction of temperatures further back in time to cover the past 650 thousand years (Siegenthaler et al., 2005; Spahni et al., 2005), revealing a good correlation between temperatures and methane concentrations (Figure 3). Some have even suggested that anthropogenic climate change will produce another planet, and the Earth will not go into another ice age until humans are removed from the surface of this planet (Hansen, 2005).

2.2. An Anthropogenic Emission Perspective

How are the effects of anthropogenic emissions on atmospheric chemical composition manifest? Figure 4 shows surface measurements of F11 (CFCl_3), methyl chloroform (CH_3CCl_3), methane, and nitrous oxide at five global background stations.

From 1978 to the end of 1980s, both CFCl_3 (Figure 4a) and CH_3CCl_3 (Figure 4b) show a persistent increase in their atmospheric concentrations with similar growth rates measured at stations across the globe; in the southern hemisphere mid latitude (Tasmania), tropical regions (American Samoa in the Pacific Ocean, and Barbados in the Atlantic Ocean), and northern hemisphere mid latitudes (Oregon, California, and Mace Head). Given the fact that more than 90% of CFCl_3 and CH_3CCl_3 have been emitted to the atmosphere from industrialised countries concentrated around North America, West Europe, and East Asia, the increases in these two species were almost the same in the globe before 1990 (Wang and Shallcross, 2001). This indicates the effectiveness of the winds in redistributing long-lived trace gases in the atmosphere. In other words, the impacts of emissions were not confined to local areas where emissions occurred. Instead, the impacts of emissions have been experienced globally. Since the signing of the Montreal Protocol in 1987, which phased out the use of these species in a variety of applications, their atmospheric concentrations have gradually reduced for CFCl_3 and significantly reduced for CH_3CCl_3 . Also, the constant hemispheric gradients of these species shown during the 1970s and 1980s have gradually reduced and hemispheric concentrations of these species have converged. This indicates the emission control of these species in the Northern Hemisphere is very effective. No additional emissions have been pumped into the Northern Hemisphere leading to the gradual convergence of the hemispheric concentrations.

The successful examples shown in regulating emissions of CFCl_3 and CH_3CCl_3 and other chlorofluorocarbons demonstrate that humans can rectify their deeds, but the impact of the CFCs on stratospheric ozone will still take most of this century to reduce to zero. Unfortunately, the controls of CO_2 emissions have been less successful than the control of chlorofluorocarbons emissions. Figure 4c shows the time evolution of the non-Montreal controlled species methane. The growth rates for methane concentrations measured at these global stations persist, and the hemispheric gradients maintained. This could indicate sustained increase in methane emissions over their source regions. Notice that atmospheric methane concentrations seem to show a trend towards stabilization in

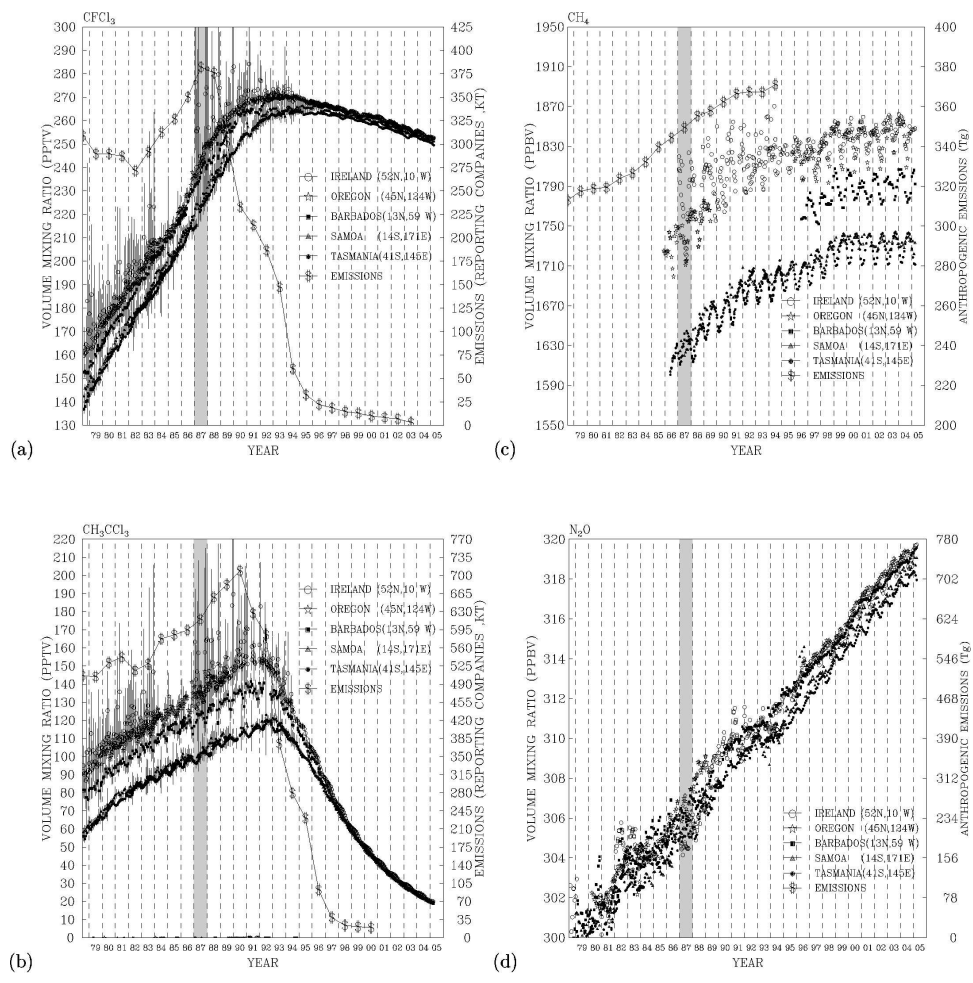


Figure 4: Atmospheric concentrations of (a) CFC₁₃, (b) CH₃CCl₃, (c) CH₄, and (d) N₂O measured at a global network of the ALE/GAGE/AGAGE stations (Prinn et al., 2000). Also superimposed on each plot is the estimated emission of each species, except N₂O. Emissions of CFC₁₃ were taken from AFEAS (www.afeas.org), CH₃CCl₃ emissions were estimated by McCulloch and Midgley (2001), and CH₄ emissions were estimated by Stern and Kaufmann. (1996). Shaded region indicates the year when the Montreal Protocol was signed.

recent years (Dlugokencky et al., 2003). It is likely that sources and sinks of atmospheric methane are now roughly balanced (Leliveld et al., 2005). Some have attributed the slow down to significant reduction in fossil fuel production over Soviet Union after the economy downturn during 1992-1993 (Wang et al., 2004). However, worldwide gas production has increased since 1990 (Leliveld et al., 2005). More detailed studies are still needed to determine the causes driving methane variations since the 1990s.

2.3. An Air Pollution Perspective

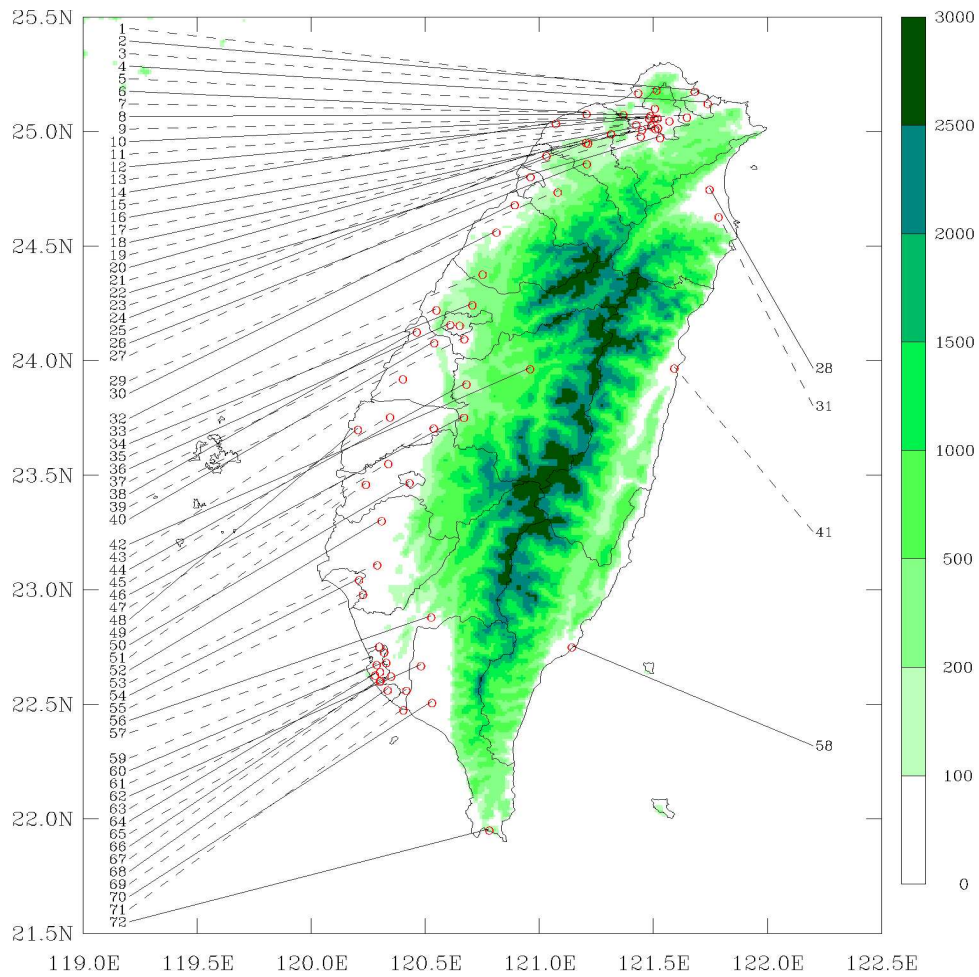


Figure 5: Spatial distributions of Taiwan EPA ambient air monitoring stations. The topography was in colors (in the units of meters).

It is well-known that Taiwan is located in one of the most energetic monsoon zones on Earth. Several studies have characterized meteorological aspects of monsoons in Taiwan and over East Asia. Most studies focused on character-

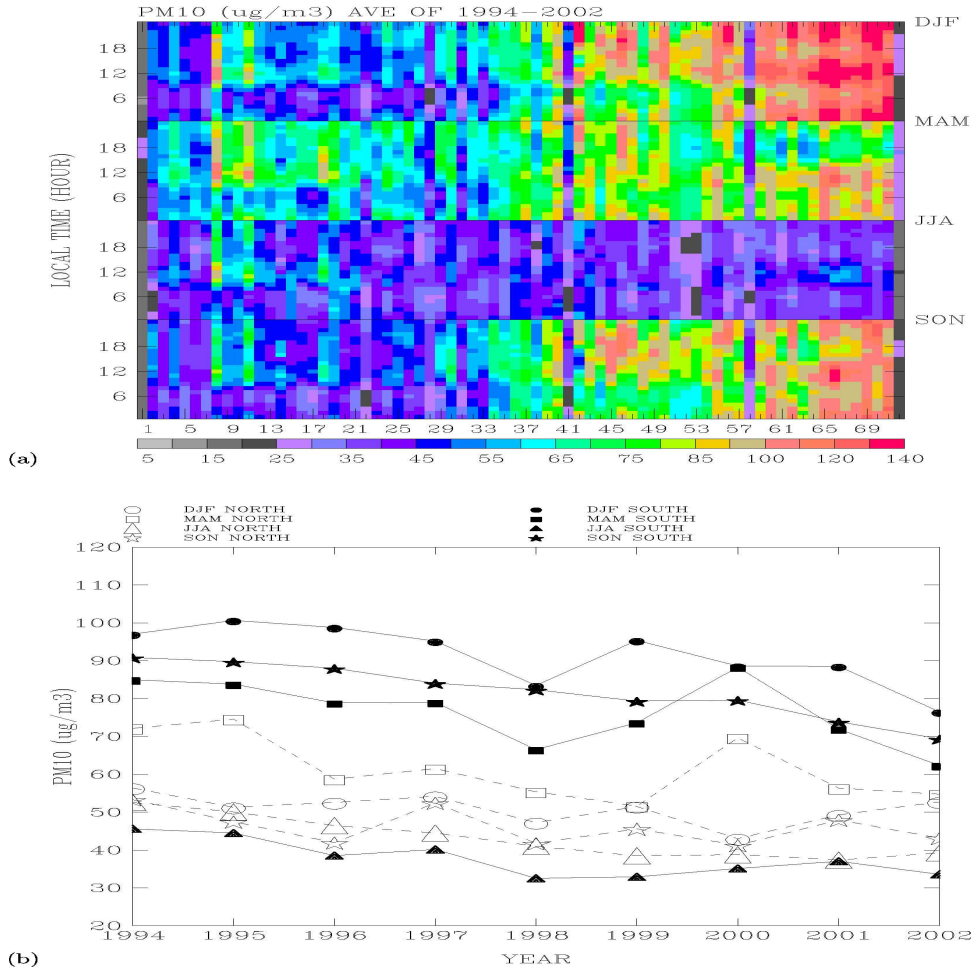


Figure 6: (a) PM_{10} ($\mu\text{g m}^{-3}$) climatology for winter (DJF), spring (MAM), summer (JJA), and autumn (SON). The x-axis shows station index as indicated in Figure 5, while y-axis indicates the local time (hour), showing the mean diurnal variation in each season at each station. (b) Seasonal and station average of PM_{10} for the period 1994-2002. Open symbols represent the means in the north, while closed symbols represent the means in the south. These plots are taken from Wang (2005).

izing rainfall associated with monsoons (e.g. Chen et al., 2002). Ambient air measurements from a network of continuous and automatic monitoring stations around the country (Figure 5) provide another rich dataset that are largely neglected by atmospheric scientists but could yield new insights into the Asian monsoon flows and their potential impacts on ground-level air pollution and rainfall distribution under the context of climate change. For example, Figure 6a shows an analysis of PM_{10} levels over Taiwan during 1994-2002 (Wang, 2005). PM_{10} are particles with a diameter of less than $10 \mu\text{m}$ and are implicated with respiratory problems in humans. Though Taiwan is not very big, about 400 km from north to south, and 150 km from west to east, ambient PM_{10} levels show distinctive seasonal variations and spatial patterns. In winter, PM_{10} levels were higher in the south and lower in the north. In winter, the entire country was covered by elevated PM_{10} levels with the south slightly higher than in the north. In summer, PM_{10} levels in the south were very low, even lower than those measured in the north. In fall, PM_{10} distributions return to the high south low north patterns seen in winter. Given the fact that anthropogenic sources of PM_{10} exhibit very little seasonal variations within a year, what causes PM_{10} to exhibit such strong seasonal variations and a reversal of north-to-south PM_{10} gradients? Notice that there are two stations in the south showing very low PM_{10} levels amid the high concentrations. These two stations, located in the east and having similar latitudes compared with their western counterparts, exhibit lower pollutant levels than the stations in the west. Figure 6b shows decreasing trends of PM_{10} in the south and in the north, respectively, during 1994-2002. In addition, some large variations in PM_{10} levels were observed during this 9-year period. In 1998, anomalously low PM_{10} levels were observed, while in 2000 anomalously high PM_{10} levels were observed in spring. Based on an analysis of airstreams in East Asia, Wang (2005) studied the changing behavior of long-range transport and their potential impact on meteorological factors controlling ground-level PM_{10} levels.

1. Motivations

The main motivations for studying atmospheric chemistry can be summarized in following points:

- What are the past and present states of atmospheric chemical composition?
- Why have there been changes in the atmospheric chemical composition?
- What are the causes for these changes?
- What are the impacts incurred by the changing atmospheric chemical composition?
- What will be the state of atmospheric chemical compositions in the future?

1. Methods

2. The IMS-Lagrangian Model

A three-dimensional (3D) Lagrangian model for idealized particle emissions and advection has been continuously developed since 1998 (Wang and Shallcross, 2000). The model was derived from the 3D integrated modelling system (IMS) and is now called the IMS-L (Lagrangian) model. The IMS-L model use winds from analysis data (e.g. NCAR/NCEP 50-year reanalysis and ECMWF ERA-15/ERA-40 data), or winds produced by other GCMs or climate simulations as input to simulate evolution of a large ensemble of particles in the atmosphere with respect to the input winds. The IMS-L model can make either forward or backward simulation in time. There is no upper limit on the total number of particles that can be simulated simultaneously except the limitations given by the computer hardware (memory). The IMS-L model has now been heavily used as a main tool to study transport and dispersion processes of pollutants in East Asia (Wang, 2005). Since the model is a global 3D model, there is no limitation on the use of this technique to other regions of interest (Wang et al., 2005).

Another frequently used global 3D particle dispersion model is called FLEXPART (Stohl et al., 1998). The US National Oceanic and Atmospheric Administration (NOAA) developed a single-particle Lagrangian model called HYSPLIT (Hybrid Single-Particle Lagrangian-Integrated Trajectory) model for trajectory calculations (e.g. Draxler and Hess, 1998). Both FLEXPART and HYSPLIT have been widely used in understanding histories of traveling air masses. With the technical breakthrough we have achieved in developing the IMS-L model, we expect more interesting discoveries will be made in this decade based on the application of this model. The IMS-L model, the FLEXPART model, and the HYSPLIT model are currently the leading models publishing results on the atmospheric transport processes under the Lagrangian framework.

1. The IMS Model

The 3D IMS model for chemistry and transport in the troposphere has been continuously developed since 1995 (Wang et al., 1999; Wang and Shallcross, 2000; Wang et al., 2001; Wang et al., 2002; Wang et al., 2004). Figure 7 is a schematic diagram showing the processes considered in the IMS model, including surface emissions of anthropogenic species and natural biogenic species (for land surface and oceans, respectively), emissions in the upper troposphere from airplanes, emissions from lightning activities, and photochemical reactions. Figure 8a shows major reaction paths for NO_x in air considered in the IMS model. The conversion of NO to NO₂ by peroxy radicals (RO₂) provides a major source for ozone production. In the nighttime, the reaction of O₃ with NO₂ gives NO₃ which is very important for nighttime chemistry. NO₂ also reacts directly with OH to form HNO₃. A typical tropospheric oxidation processes for an organic compound such as methane is shown in Figure 8b. Once emitted into the atmosphere, methane reacts with OH, followed by reactions with O₂ to give CH₃O₂, which converts NO to NO₂ and leads to the photochemical production of ozone. Photolysis of ozone produces some excited state oxygen atoms that

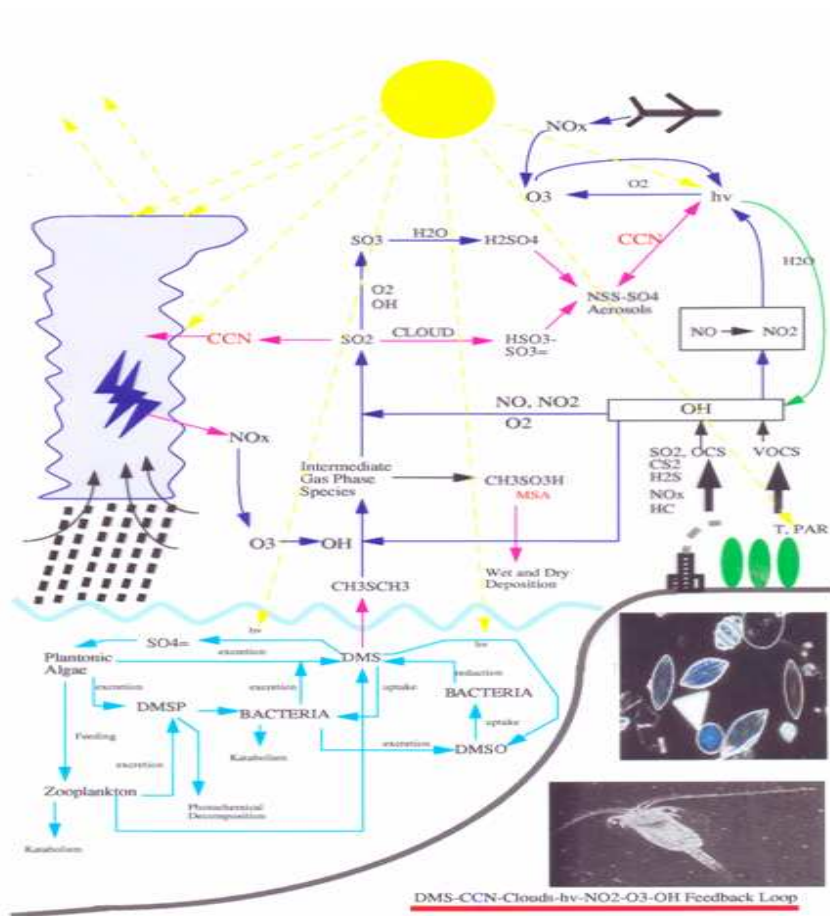
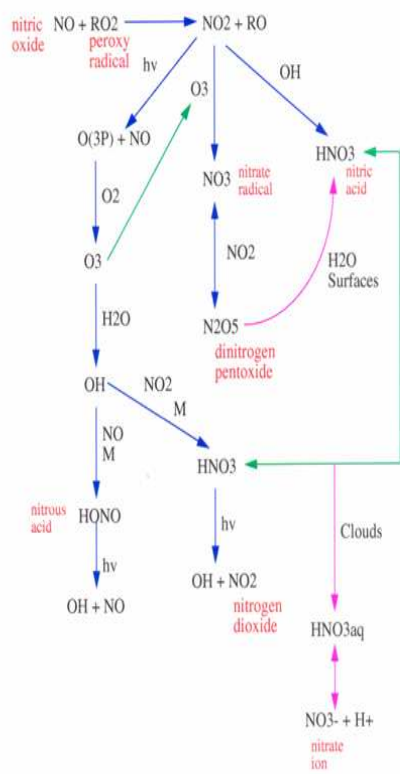


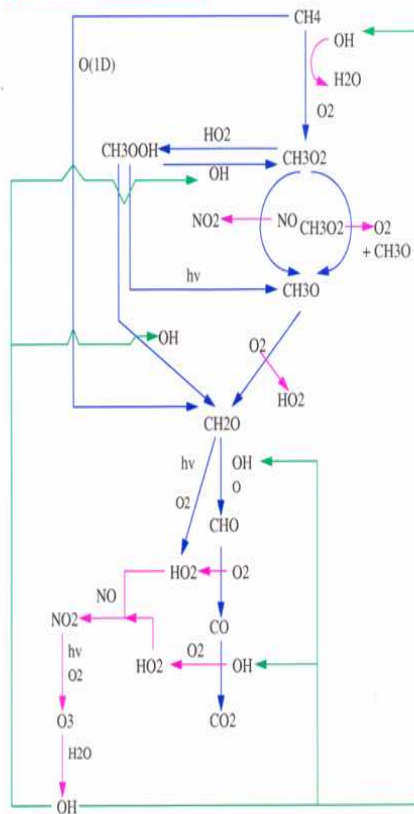
Figure 7: A schematic diagram showing emissions, chemistry, cloud processes, and air-sea interaction processes considered in the IMS model. This figure is taken from Wang and Shallcross (2000).

Major Reaction Paths for NO_x in Air



(a)

CH₄-CO-OH-O₃ Photochemistry



(b)

Figure 8: (a) Left panel, showing major reaction paths for NO_x in air. (b) Right panel, showing CH₄ oxidation paths in the troposphere.

can react with water vapour to form OH radicals. Hence the production of ozone will lead to the production of OH radicals.

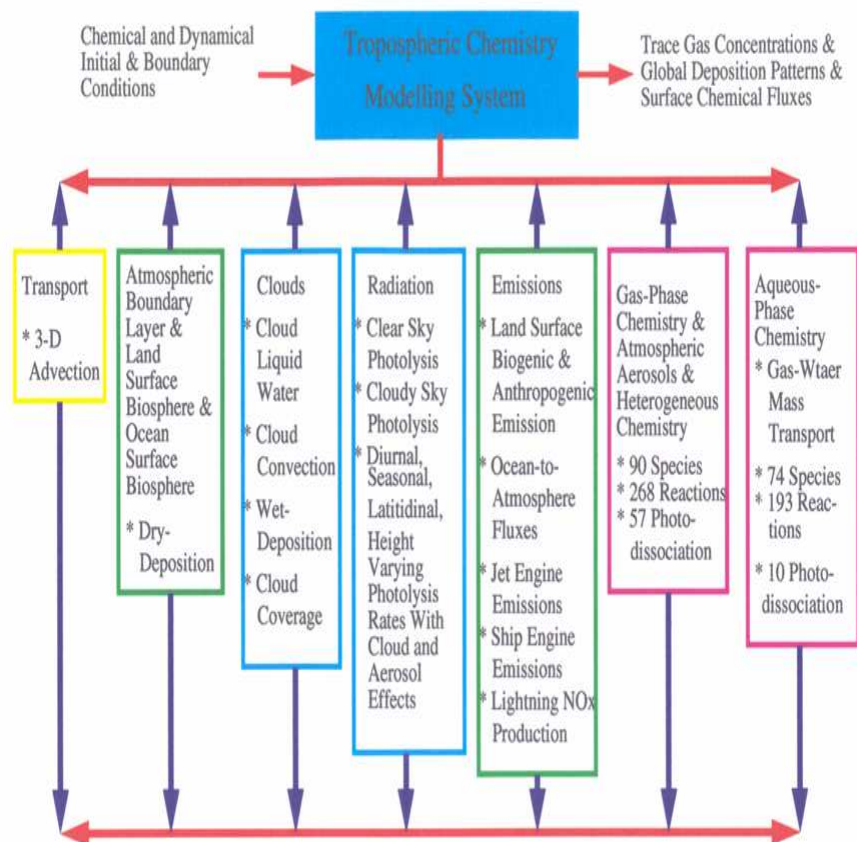


Figure 9: A diagram showing the computational modules considered in the IMS model.

Figure 9 is a schematic diagram showing the main structures of the IMS model. The model considers 3D advection of long-lived species, atmospheric boundary layer processes (land surface processes, chemical exchange processes between air and the oceans, and dry deposition processes), cloud processes (cloud convections, cloud droplet and cloud rain drops, and wet deposition processes), atmospheric radiation (clear and cloudy sky radiation, and calculations of photolysis rates as a function of latitude, altitude and season), emissions (surface emissions from land vegetation and oceanic biota, anthropogenic emissions from surface and in the troposphere, and lightning production of NO_x species), gas-phase chemistry, and aqueous-phase chemistry. The model has been designed to run efficiently on multi-tasked share-memory platform such as CRAY

J90 supercomputer (Wang et al., 2000). We are now working on a new version of the IMS model so that it can be run on distributed memory platforms (such as PC clusters). We have used the NCAR/NCEP 50-Year reanalysis data to run the IMS model for the period 1948-2003. Two separated integrations have been completed: The IMS-20 integration (1984-2003), and the first the IMS-55 integration (1948-1978). Some results from the IMS-20 integration will be shown in the following chapter.

1. Chemistry Box Models

A generalised organic/NOx mechanism (after Seinfeld and Pandis (1998))

	Reaction	Rate constant (298 K)
R1	$\text{NO}_2 + \text{h}\nu \rightarrow \text{NO} + \text{O}$	$8.9 \times 10^{-3} \text{ s}^{-1}$
R2	$\text{O} + \text{O}_2 + \text{M} \rightarrow \text{O}_3 + \text{M}$	$6.0 \times 10^{-34} \text{ cm}^6 \text{ molecule}^{-2} \text{ s}^{-1}$
R3	$\text{O}_3 + \text{NO} \rightarrow \text{NO}_2 + \text{O}_2$	$1.8 \times 10^{-14} \text{ cm}^3 \text{ molecule}^{-1} \text{ s}^{-1}$
R4	$\text{RH} + \text{OH} \rightarrow \text{RO}_2 + \text{H}_2\text{O}$	$26.3 \times 10^{-12} \text{ cm}^3 \text{ molecule}^{-1} \text{ s}^{-1}$
R5	$\text{HCHO} + \text{h}\nu \rightarrow 2\text{H}_2 + \text{CO}$	$2.96 \times 10^{-5} \text{ s}^{-1}$
R6	$\text{HCHO} + \text{h}\nu \rightarrow \text{H}_2 + \text{CO}$	$4.25 \times 10^{-5} \text{ s}^{-1}$
R7	$\text{HCHO} + \text{OH} \rightarrow \text{HO}_2 + \text{CO} + \text{H}_2\text{O}$	$9.37 \times 10^{-12} \text{ cm}^3 \text{ molecule}^{-1} \text{ s}^{-1}$
R8	$\text{RCHO} + \text{OH} \rightarrow \text{RCOO}_2 + \text{H}_2\text{O}$	$15.8 \times 10^{-12} \text{ cm}^3 \text{ molecule}^{-1} \text{ s}^{-1}$
R9	$\text{RO}_2 + \text{NO} \rightarrow \text{NO}_2 + \text{RO}$	$8.9 \times 10^{-12} \text{ cm}^3 \text{ molecule}^{-1} \text{ s}^{-1}$
R10	$\text{RCOO}_2 + \text{NO} \rightarrow \text{NO}_2 + \text{RO}_2 + \text{CO}_2$	$2.4 \times 10^{-11} \text{ cm}^3 \text{ molecule}^{-1} \text{ s}^{-1}$
R11	$\text{RO} + \text{O}_2 \rightarrow \text{RCHO} + \text{HO}_2$	$1.9 \times 10^{-15} \text{ cm}^3 \text{ molecule}^{-1} \text{ s}^{-1}$
R12	$\text{HO}_2 + \text{NO} \rightarrow \text{NO}_2 + \text{OH}$	$8.6 \times 10^{-12} \text{ cm}^3 \text{ molecule}^{-1} \text{ s}^{-1}$
R13	$\text{O}_3 + \text{h}\nu \rightarrow \text{O}_2 + \text{O}(^1\text{D})$	$3.65 \times 10^{-5} \text{ s}^{-1}$
R14	$\text{O}(^1\text{D}) + \text{H}_2\text{O} \rightarrow 2\text{OH}$	$2.2 \times 10^{-10} \text{ cm}^3 \text{ molecule}^{-1} \text{ s}^{-1}$
R15	$\text{OH} + \text{NO}_2 + \text{M} \rightarrow \text{HNO}_3 + \text{M}$	$1.15 \times 10^{-11} \text{ cm}^3 \text{ molecule}^{-1} \text{ s}^{-1}$
R16	$\text{HO}_2 + \text{HO}_2 \rightarrow \text{H}_2\text{O}_2 + \text{O}_2$	$5.02 \times 10^{-13} \text{ cm}^3 \text{ molecule}^{-1} \text{ s}^{-1}$
R17	$\text{RO}_2 + \text{HO}_2 \rightarrow \text{ROOH} + \text{O}_2$	$5.6 \times 10^{-12} \text{ cm}^3 \text{ molecule}^{-1} \text{ s}^{-1}$
R18	$\text{RCOO}_2 + \text{NO}_2 + \text{M} \rightarrow \text{PAN} + \text{M}$	$8.69 \times 10^{-12} \text{ cm}^3 \text{ molecule}^{-1} \text{ s}^{-1}$
R19	$\text{PAN} \rightarrow \text{RCOO}_2 + \text{NO}_2$	$5.2 \times 10^{-4} \text{ s}^{-1}$
R20	$\text{HO}_2 + \text{O}_3 \rightarrow \text{OH} + 2\text{O}_2$	$2.0 \times 10^{-15} \text{ cm}^3 \text{ molecule}^{-1} \text{ s}^{-1}$

Figure 10: A generalized organic/NOx reaction mechanism. This figure is taken from Wang et al. (2003).

In addition to the very complicated 3D chemistry model described above, chemistry box models have been developed to study chemistry data assimilation

in the stratosphere (Wang et al., 2001) and urban air pollution in the troposphere (Wang et al., 2002). Box models are ideal for testing hypotheses and gaining insight into the photochemical theory. Figure 10 shows an example of a photochemical reaction mechanism used to study urban air pollution. We have started applying this modelling technique to study urban air pollution over Taiwan. The ambient air measurements can be best understood if we can systematically apply photochemical theory through these data. Some results will be shown in the following chapter.

1. High-Performance Clusters

Given the immense capability in making advanced PC hardware by Taiwan's world-leading computer industry, it will be a tremendous benefit for us if we can build high performance platforms based on these high quality PCs developed and built in Taiwan. With this in mind, we built our first generation of PC clusters DOBSON to run models for high resolution environmental modeling over Taiwan and East Asia regions (Wang et al., 2005). The DOBSON cluster is a 16-node SMP PCs built on the Intel Pentium III 1 GHz CPUs. The DOBSON runs Linux RedHat 7.2 operating system. The second generation cluster called BOROK, which was built based on 4 nodes of Intel Xeon 3.2 GHz SMPs, 2 nodes of Intel Pentium III 1 GHz SMPs, 1 node of AMD PC, and 1 node of Intel Pentium IV 3 GHz PC. The BOROK cluster runs Linux Fedora Core 2 operating system. We are now building the third generation cluster Cajal. It will be difficult to run simulations with spatial resolutions at 1-km or less over entire Taiwan without using a high performance computation platform. Since funding for computer resources is significantly under appreciated than funding for field experiments in Taiwan, we need to find innovative ways to build our own computational capability.

1. Modelling Long-range Transport of Asian Pollutants

5.1. The Classic April 1998 Trans-Pacific Long-range Transport

The most active season for long-transport of pollutants from the Asian continent to the Pacific occurs during the spring season. Natural sources of pollutants include wind-blown dust from the Gobi and Takalamakan deserts and biomass burning smoke originating from south-east Asia and the Siberian regions. Figure 11 shows a classic example of long-range transport of Asian desert dust crossing the North Pacific to reach North American during 19-26 April 1998 (e.g. Uno et al., 2001). This is the first satellite observation of long-range transport of continental dust across the entire length of the Pacific Ocean to be published (Huntrieser et al., 2005). The TOMS satellite data vividly captured a 7-day sequence of the trans-North Pacific transport of the dust as it emerged from northeast China, leaving the Asian continent, passing Korea and crossing Japan, approaching and passing the International Date line, and reaching the western coast of North America. We have run the IMS-L model to see if we can reproduce the April 1998 trans-Pacific transport event. The idealized particles

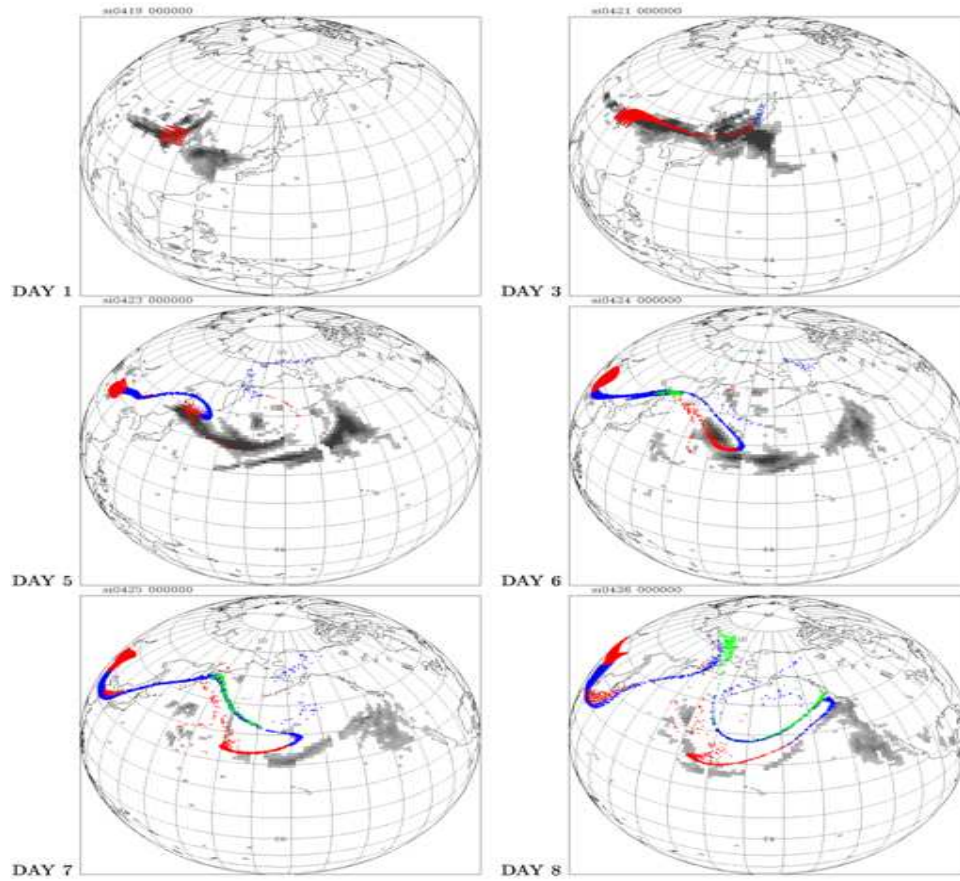


Figure 4. Case 9804.

Figure 11: The IMS-L simulations of trans-Pacific long-range transport of particles (colored), and the TOMS AI measurements during 19 (DAY 1) – 26 (DAY 8) of April 1998. Particle altitudes less than 3 km were colored red, between 3-6 km were colored blue, higher than 6 km were colored green.

were emitted at the surface over the Gobi area, and were continuously emitted over the following 7-day period. Figure 11 compares model simulation of particles with TOMS aerosol index (AI). The similarity between TOMS AI and model particles during the trans-Pacific process indicates that the large-scale winds were the process responsible for carrying the Asian pollutants crossing the North Pacific. In this event, it took about 7 days for Asian pollutants to impact North America. This leads to the possibility for building an early warning system for the long-range transport of Asian pollutant to North America. If we are able to reproduce large-scale winds reasonably close to the observed winds, we should be able predict the movement of emerging Asian pollutants when they appear on the satellite remote sensing measurements.

5.2. The April 2001 Dust Storm of the Century

Simulation of Asian Dust events of April 2001

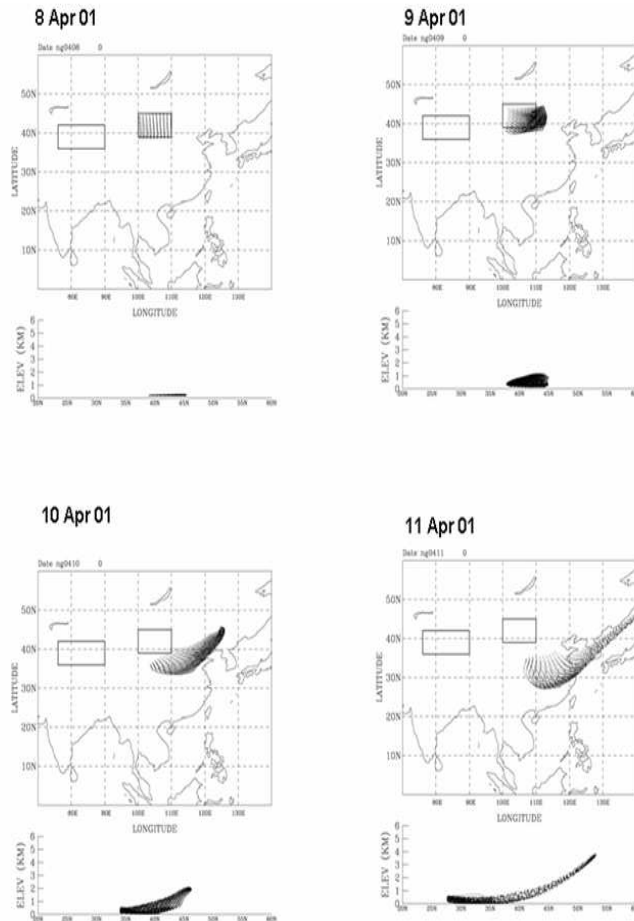


Figure 12: Simulation of Asian dust events of April 2001. Right box indicates Gobi region, and left box indicate Taklamakan region.

Gobi Source

Taklamakan Source

EPA Measurements

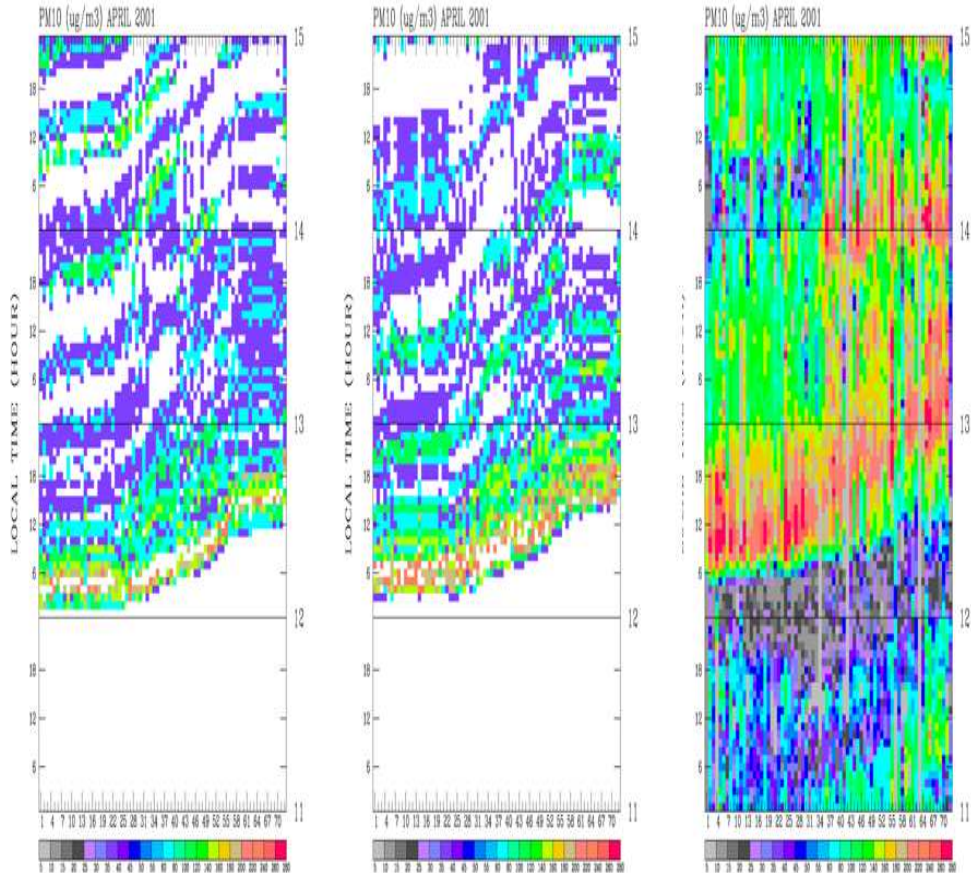


Figure 13: (Right panel) PM_{10} measurements during 11-14 April 2001. The x-axis indicates EPA station indices (as shown in Figure 5), while the y-axis indicate hour. (Central panel) Modeled PM_{10} concentrations with respect to emission sources from Taklamakan regions were considered. (Left panel) The same as in central panel but with respect to emission sources from Gobi region. This figure is taken from Wang [2007].

While the April 1998 trans-Pacific transport is a classic example of the eastward long-range transport of emerging Asian pollutants, the event that occurred during 8-12 April 2001 showed one of the most significant southward transport events of emerging Asian pollutants. Figure 12 shows a model simulation of a series of particle distributions after their emissions from the Gobi region on 8 April 2001. Notice that particles were emitted at the surface and their subsequent transport in the atmosphere were entirely determined by meteorology. On 9 April, these particles were transported eastward, then, on 10 April, transported southward. On 11 April, the particle front gradually approaching northern Taiwan from the East China Sea. These particles passed over the entire length of Taiwan on 12 April 2001. Figure 13 shows a space-time plot of hourly PM_{10} measured at 72 EPA ambient stations. A pronounced high PM_{10} event was observed on April 2001. The event started at about 06:00 am, where the stations in northern Taiwan first picked up anomalously high PM_{10} levels. These high PM_{10} levels then systematically moved through central Taiwan to finally reach stations in southern Taiwan as the day went on. Figure 13 also shows model particle concentrations passing these EPA stations. The characteristic pattern of PM_{10} sweeping cross Taiwan, as shown in the observations, is very nicely reproduced by the model. The model shows that pollutants with both Gobi and Taklamakan origins made contributions to this significant long-range transport of dust event. It is very rare that dust from Taklamakan can reach latitudes as south as over Taiwan (Sun et al., 2001). The April 2001 event is a classic case showing that, when this did happen, the joint pollutants from the Gobi and the Taklamakan can produce a significant natural pollution event. Our simulations also show that the EPA measurements are valuable for identifying long-range transport of emerging Asian pollutants.

5.3. Long-range Transport of Biomass Burning Smoke

Another important source for long-range transport of emerging Asian pollutants is from biomass burning smoke. Figure 14 shows a sequence of 12 days of TOMS AI data over southeast and east Asia, and the simulation of particle distribution using the IMS-L model during the same period. Our IMS-L simulations show that the spatial distribution of particles closely resemble the spatial distribution of the burning smoke, as shown in the elevated levels of AI data. This indicates that the temporal and spatial distribution of the burning smoke is controlled by the large scale winds. Hence, if we know where fires are, and know the winds, then we should be able to predict the long-range distribution of biomass burning smoke. On 20 March 1998 (Figure 15a), heavy smoke (indicated by dark colored AI values) covered the entire Taiwan area. Inspection of the ozonesonde data on this day (Figure 15c) shows an increase in ozone concentrations from 2 km (~ 70 ppbv) to 4 km (~ 140 ppbv). On this day, Taiwan was blanked by elevated TOMS AI values, and modeled particles appear at an altitude close to 4 km to the north and about 2 km to the south. Hence, Taiwan was bounded by particles, emitted from south-east Asia and were transported to Taiwan at 4 km in altitude to the north and at about 2 km in altitude to the south. The altitudes of these particles are consistent with the altitudes of the ozonesonde data where peak ozone concentrations were observed. Hence the 2-4

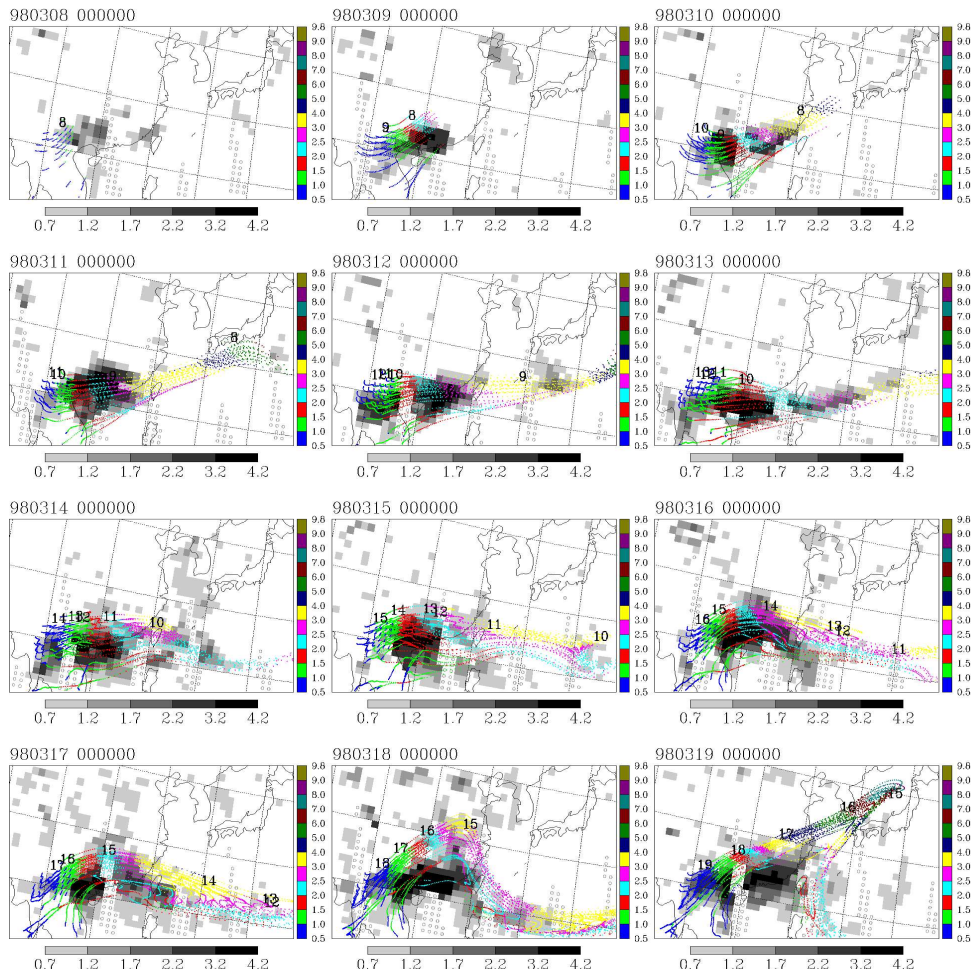


Figure 14: Simulation of the Southeast Asia biomass burning events occurred during 8-20 March 1998. The TOMS AI data were colored grey, while the particle distributions were colored based on their altitudes (in the units of km).

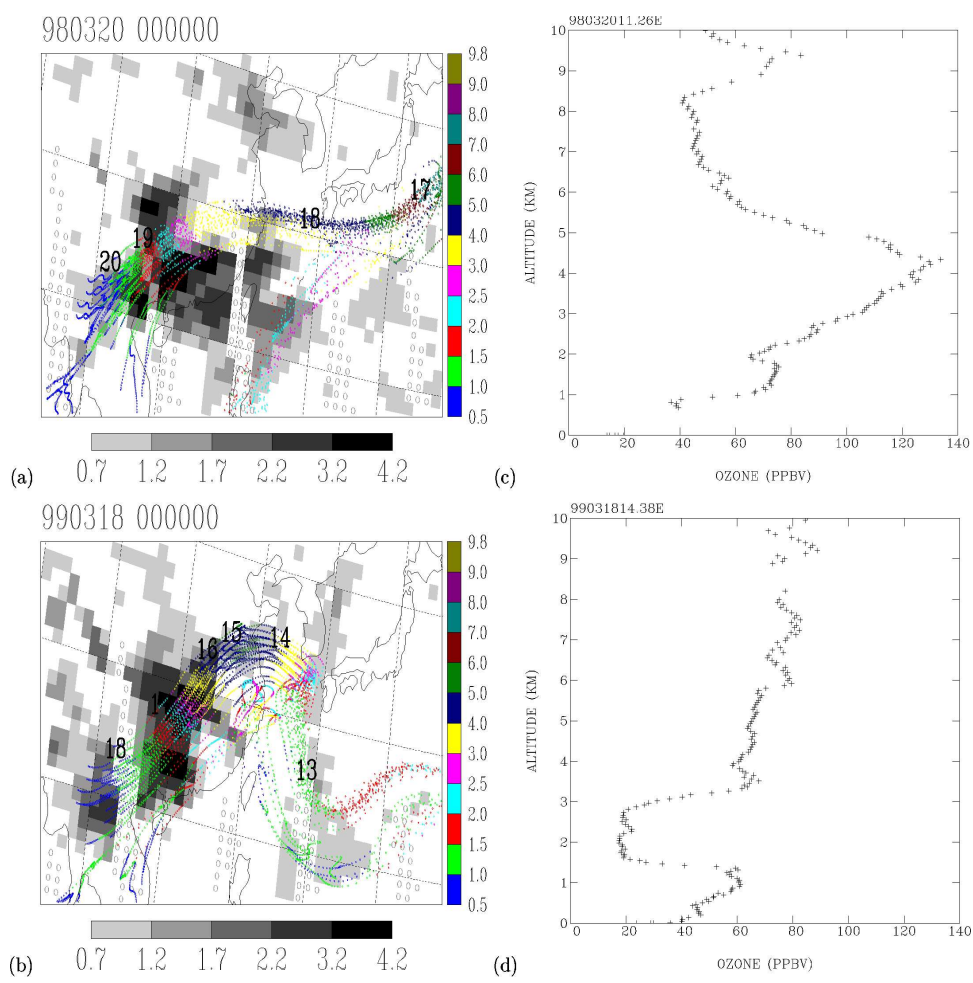


Figure 15: Biomass burning simulations on (a) 20 March 1998 and (b) 18 March 1999. Ozonesonde profiles over Taipei on (c) 20 March 1998 and (d) 18 March 1999.

km increase in ozone was due to the long-range transport of biomass burning smoke which transports ozone precursors and/or ozone over Taiwan region. One very significant point from this simulation is that, since TOMS AI data gives us only a 2D distribution of aerosol and no information in the vertical can be obtained, our IMS-L simulations show that the smoke is likely to prevail over the 2-4 km altitude as revealed in the altitudes of the particles.

The IMS-L model was also used to simulate long-range transport of the 1999 biomass burning smoke over Southeast and East Asia (not shown here). Again, during the 12 days of smoke captured by the TOMS AI data, the IMS-L model produces particle distributions that closely resemble TOMS data. On 18 Mar 1999 (Figure 15b), no TOMS AI values appear over Taiwan. The IMS-L simulation shows that particles appear over northern Taiwan and at altitudes between 1 and 1.5 km. The ozonesonde data (Figure 15d) show that a pronounced dip of ozone concentrations from close to 1 km (~ 60 ppbv) to about 1.5 km (~ 20 ppbv). Low ozone concentration close to 20 ppbv appears in the altitudes between 1.5 and 3 km. Hence, the IMS-L simulation shows that low ozone concentrations shown in this narrow range of about 1-2 km thickness of air was most likely due to the northward intrusion of clean air from low tropical latitudes.

These analyses show that ozone vertical structure is very complicated and these ozone laminar structures can be understood when the IMS-L model simulations were combined with the TOMS AI data.

1. Modeling Tropospheric Chemistry: The IMS-20 Integration

Detailed studies of tropospheric chemistry using the IMS model were reported in Wang et al. (1999), Wang and Shallcross (2000), Wang et al. (2001), Wang and Shallcross (2002), and Wang et al. (2004). In these works, the IMS simulations were run for an entire year to study seasonal variations of tropospheric chemistry. Given the importance of the chemistry-climate interactions described above, long-term climate integrations with interactive chemistry feedback processes included are necessary for the next generation climate impact assessment (Wong et al., 2004; Wang et al., 2004; Wang and Shallcross, 2005). Here we conduct a long-term integration of the IMS model for the period 19984-2003. In this simulation, we use winds from the NCEP/NCAR 50-Year Reanalysis data.

Figure 16 shows a simulation of monthly mean ozone at Mauna Loa and the comparison with measurements. The strong seasonal cycle of ozone at this site is in general closely reproduced by the model. This indicates that the main process governing ozone variation is basically reproduced by the model. In a separate work (not shown here), we found that the stratosphere-troposphere exchange process is a very important process for ozone concentrations over Mauna Loa. The measurements at Mauna Loa not only show seasonal ozone cycles, these data also reveal inter-annual variations of ozone. For example, an increasing trend of ozone from 1989 to 1993, followed by decreasing trend from 1993 to 1995, and another increasing trend from 1995 to 1998. The inter-annual variations from 1993 to 1998 were generally reproduced by the model, though the

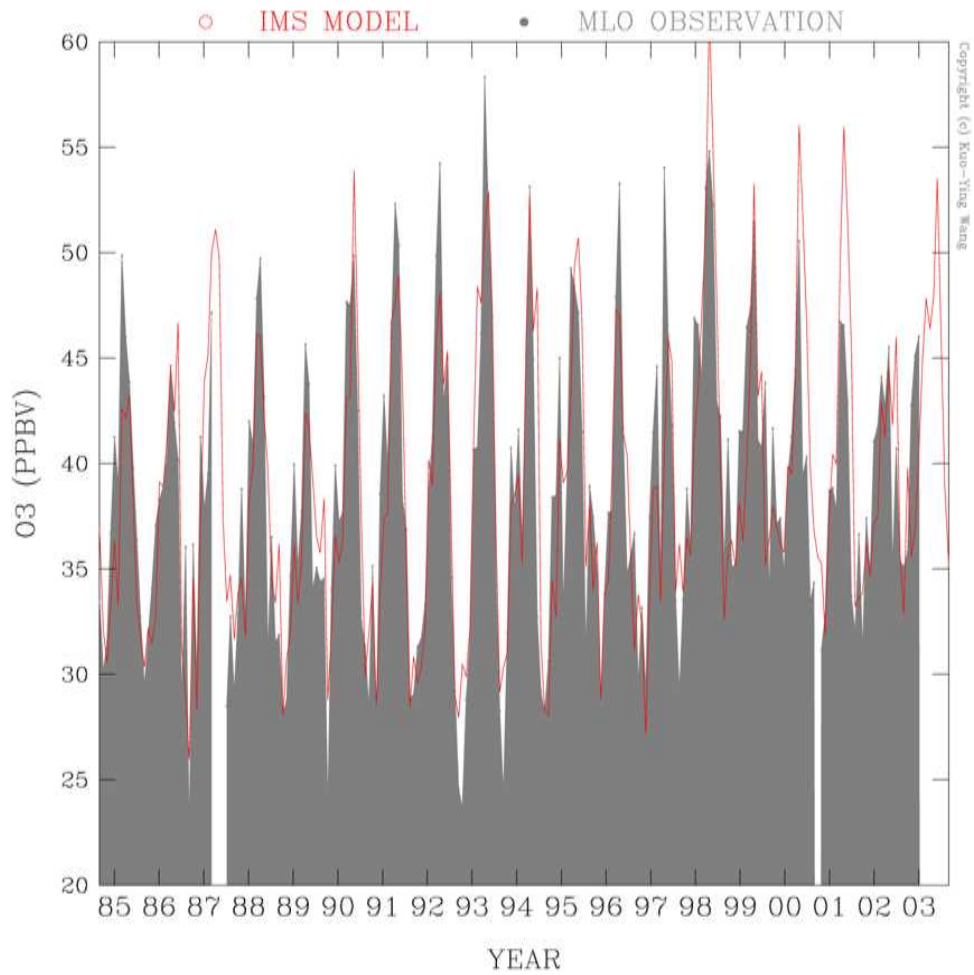


Figure 16: The IMS simulation of monthly mean surface ozone (ppbv) at Mauna Loa for the period 1984-2003 (colored red). The measured monthly mean surface ozone concentrations for the same period were colored in grey.

model under-predicts peak ozone concentrations in 1996 and 1997, and over-predicts ozone concentrations in 1998. The model also over-predicts peak ozone in 2000 and 2001. The low ozone in 2002 compared with high ozone peaks in 2001 and 2003 is well reproduced.

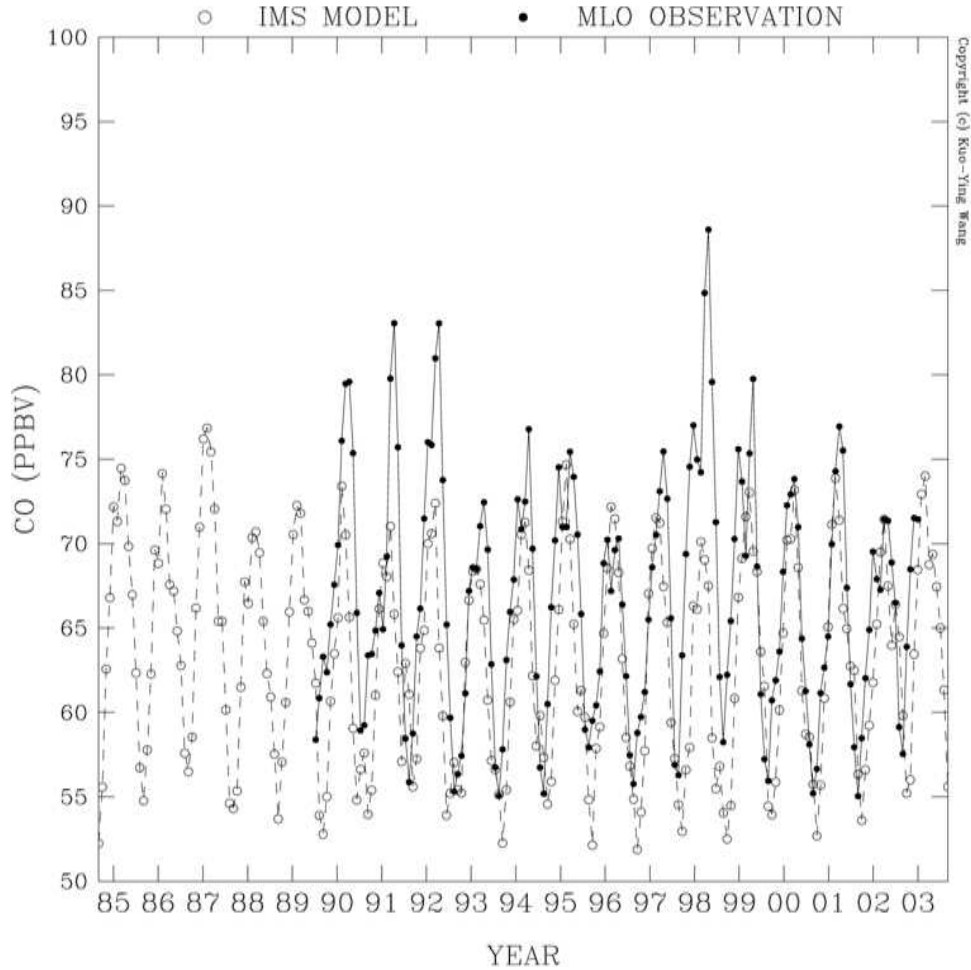


Figure 17: The IMS simulation of monthly mean surface CO (ppbv) at Mauna Loa for the period 1984-2003 (open circles). The measured monthly mean surface CO concentrations for the same period were shown in solid circles.

Figure 17 shows a comparison of CO between model simulation and measurements. Strong seasonal cycles of CO shown in the measurements were generally reproduced by the model, for example, during the periods 1993-1997 and 1999-2002. High CO concentrations in 1990, 1991, 1992, and 1998 were under-predicted by the model. Since the model used a fixed biomass burning emission rate for the period 1984-2003, inter-annual variability in biomass burning activities were not accounted for. The 1997/1998 period is the biggest ENSO

recorded for the 20th century. Recorded biomass burning events occurred over Tropical Indonesia (e.g. Page et al., 2002).

Our comparisons of ozone and CO over Mauna Loa show that the model is ideal for understanding long-term measurements. These experiments reveal new questions on tropospheric chemistry when considered in a climate context. These comparisons also expose new directions for further model developments.

1. Summary

Modeling is a very important tool for scientific process, requiring long-term dedication, desire, and continuous reflection. In this work, we discuss several aspects of modeling, and the reasons for doing it. We discuss two major modeling systems that have been built by us for the past 10 years. It is a long and arduous processes but the reward of understanding can be enormous, as demonstrated in the examples shown in this work. We found that long-range transport of emerging Asian pollutants can be interpreted using a Lagrangian framework. More detailed processes still need to be modeled but an accurate representation of meteorology is the most important thing above others. Our long-term chemistry integrations reveal the capability of simulating tropospheric chemistry on a climate scale. These long-term integrations also show ways for further model development.

Modeling is a quantitative process, and the understanding can be sustained only when theories are vigorously tested in the models through comparison with measurements. We should also not over look the importance of data visualization techniques. Humans feel more confident when they see things. Hence, modeling is an incredible journey, combining data collection, theoretical formulation, detailed computer coding and harnessing computer powers.

1. Some Future Directions

8.1. Modeling Air Pollution

Modeling air pollution is a grand challenge. Compared with operational daily weather prediction, operational daily air pollution prediction is still in its infancy. We have built an air pollution box model, based on the chemical reaction mechanism described in Wang et al. (2002), to understand EPA measurements. Figure 18 shows an 18-hour simulation of hourly ozone concentrations over Bingdong in the southern Taiwan on 29 July 1995. The measurements show a two-peak ozone pattern, one centered about the noon time, and the other one centered about 5:00 pm in the afternoon. The model calculates ozone concentrations that closely resemble measurements. It would be difficult to understand the measurements without detailed modeling. The calculation shows that photochemistry is the key for ozone variations on this day. We are now working on the development of this box model and to test its validity over other urban areas.

8.2. Long-Range Transport of Emerging Asian Pollutants Before 1994

./2005-EPA-Data/59 bingdong/1995/bingdong 19950729

RED- EPA DATA

BLACK- MODEL

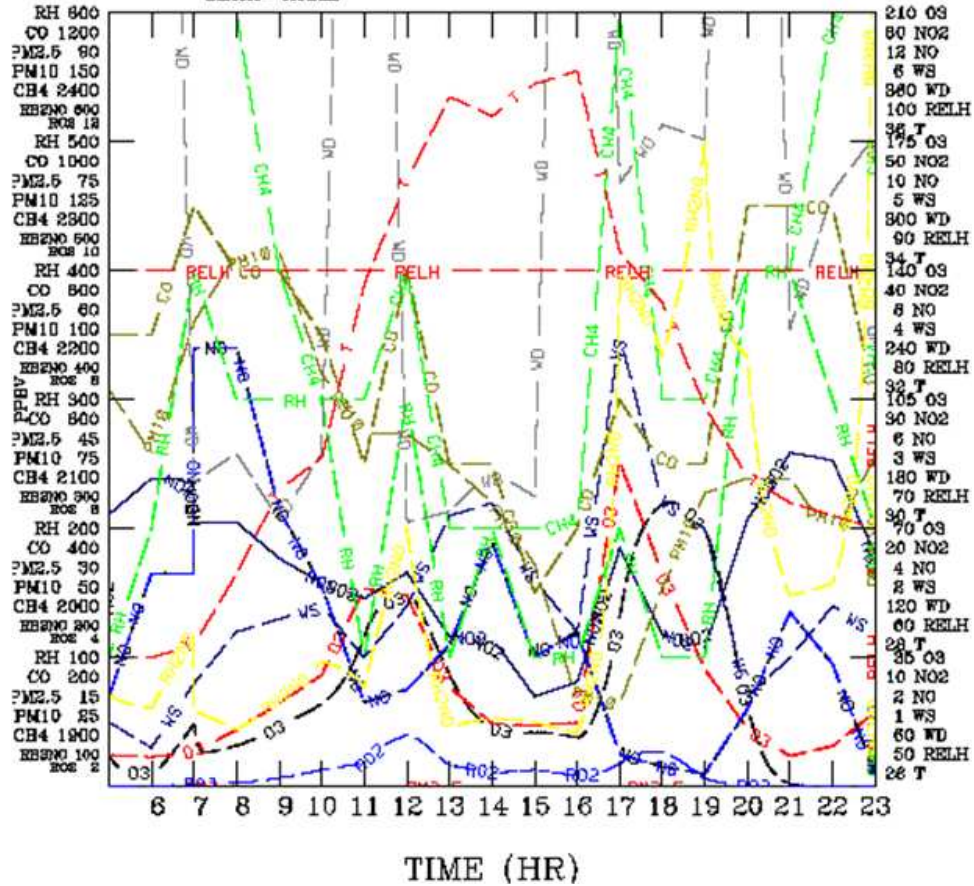


Figure 18: Air pollution box model simulations of hourly ozone concentrations (ppbv, shown in dashed red color and denoted by O3). The measured hourly ozone were colored in dashed black and denoted by O3. Ambient measurements of other species and meteorology were shown in various colors. The ozone levels were determined by the y-axis shown in the right (denoted by 35 O3, 70 O3, etc, means ozone concentrations at 35 ppbv, 70 ppbv, etc).

Work is currently in progress to apply a modeling technique, combining IMS-L simulation and EPA measurements, to calibrate long-range transport of emerging Asian pollutants during 1994-2005. This calibration will help us identify events of long-range transport during the period 1948-1994 when ambient measurements were very limited.

8.3. Lightning and Convective Activities on Chemistry Over Taiwan

Wang and Liao (2006) discussed lightning activity over Taiwan during the passing of a typhoon in July 2004. From analyses of lightning data for the period 1989-2005, significant lightning activity generally prevails during late spring, summer, to early fall seasons. It remains unknown as to what extent these lightning can impact on chemical compositions over Taiwan.

8.4. Build to Model

Why are some countries (e.g., the USA) willing to share their models with other nations while other countries maintain a more secretive attitude toward the models they build? In a stark comparison, in the pharmaceutical industry, the formula for a block-buster drug is often staunchly protected under various patents. The ability to build models is completely different compared with the ability to run and interpret models. While we may feel comfortable using models and seeing results, our ability to cultivate hands-on experience in building models from scratch has been gradually eroded. The very easy accessibility of models on the public domain may have effectively suppressed our desire to build our own models. A nation should not rely on other nations for key technological know-how (NRC, 2001). We should take notes on the lessons brought forward by Taiwan's auto industry, while the success of Taiwan's computer industry reminds us what we can achieve if we chose to do so.

Acknowledgements

The authors are very grateful to the Taiwan National Science Council for its continuous support on the Atmospheric Chemistry Modelling Laboratory at NCU. We thank H.-H. Hsu for pointing out the usefulness of the TOMS AI data, and W.-S. Kau for kindly supporting our modeling efforts on the NTU CRAY J90. We acknowledge the use of data from CWB and EPA. Many colleagues at NCU and NTU continuously provide us with insightful discussions and comments.

References

CCSP (2001), Strategic plan for the US Climate Change Science Program, A Report by the Climate Change Science Program and the Subcommittee on Global Change Research, Climate Change Science Program Office, Washington, DC 20006, USA.

Chen, T.-C., S.-Y. Wang, W.-R. Huang, and M.-C. Yen (2002), Variation of the Asian summer monsoon rainfall, *J. Climate*, 17, 744-762.

Cyranoski, D. (2004), A seismic shift in thinking, *Nature*, 431, 1032-1034.

Dlugokencky, E.J., S. Houweling, L. Bruhwiler, K.A. Masarie, P.M. Lang, J.B. Miller, and P.P. Tans (2003), Atmospheric methane levels off: Temporary pause or a new steady-state?, *Geophys. Res. Lett.*, 30(19), 1992, doi:10.1029/2003GL018126.

- Draxler, R.R., and G.D. Hess (1998), An overview of the Hysplit-4 modeling system for trajectories, dispersion, and deposition, *Aus. Meteorol. Mag.*, 47, 295-308.
- Hansen, J. (2005), Ice ages as history, *Science*, 310, 1900.
- Held, I (2005), The gap between simulation and understanding in climate modeling, *Bull. Amer. Meteor. Soc.*, 86, 1609-1614.
- Huntrieser, H., et al. (2005), Intercontinental air pollution transport from North America to Europe: Experimental evidence from airborne measurements and surface observations, *J. Geophys. Res.*, 110, D01305, doi:10.1029/2004JD005045.
- Jackson, E.A. (1991), *Perspectives of nonlinear dynamics*, Cambridge University Press, Cambridge, UK.
- Jozel, J., N.I. Barkov, J.M. Barnola, M. Bender, J. Chappellaz, C. Genthon, V.M. Kotlyakov, V. Lipenkov, C. Lorius, J.R. Petit, D. Raynaud, G. Raisbeck, C. Ritz, T. Sowers, M. Stievenard, F. Yiou, and P. Yiou (1993), Extending the Vostok ice-core record of palaeoclimate to the penultimate glacial period, *Nature*, 364, 407-412.
- Leliveld, J., S. Lechtenböhmer, S.S. Assonov, C.A.M. Brenninkmeijer, C. Dienst, M. Fishedick, and T. Hanke (2005), Low methane leakage from gas pipelines, *Nature*, 434, 841-842.
- McCulloch A., and P.M. Midgley (2001), The history of methyl chloroform emissions: 1951-2000, *Atmos. Environ.*, 35(31), 5311-5319.
- NRC (2001), *Improving the effectiveness of U.S. climate modeling*, National Academy Press, 128pp.
- Page, S.E., F. Siegert, J.O. Rieley, H.-D. V. Boehm, A. Jaya, and S. Limin (2002), The amount of carbon released from peat and forest fires in Indonesia during 1997, *Nature*, 420, 61-65.
- Prinn, R. G., R. F. Weiss, P. J. Fraser, P. G. Simmonds, D. M. Cunnold, F. N. Alyea, S. O'Doherty, P. Salameh, B. R. Miller, J. Huang, R. H. J. Wang, D. E. Hartley, C. Harth, L. P. Steele, G. Sturrock, P. M. Midgley, A. McCulloch (2000), A history of chemically and radiatively important gases in air deduced from ALE/GAGE/AGAGE, *J. Geophys. Res.*, 105(D14), 17751-17792, 10.1029/2000JD900141.
- Siegenthaler, U., T.F. Stocker, E. Monnin, D. Lüthi, J. Schwander, B. Stauffer, D. Raynaud, J.-M. Barnola, H. Fischer, V. Masson-Delmotte, and J. Jouzel (2005), Stable carbon cycle- Climate relationship during the late pleistocene, *Science*, 310, 131-1317.
- Spahni, R., J. Chappellaz, T.F. Stocker, L. Loulergue, G. Hausammann, K. Kawamura, J. Flückiger, J. Schwander, D. Raynaud, V. Masson-Delmotte, and J. Jouzel (2005), Atmospheric methane and nitrous oxide of the late Pleistocene from Antarctic ice cores, *Science*, 310, 1317-1321.
- Stern, D.I., and R.K. Kaufmann. (1996), Estimates of global anthropogenic methane emissions 1860-1993. *Chemosphere*, 33, 159-76.
- Stohl, A., M. Hittenberger, and G. Wotawa (1998), Validation of the Lagrangian particle dispersion model FLEXPART against large scale tracer experiment data, *Atmos. Environ.*, 32, 4245-4264.

Sun, J., M. Zhang, and T. Liu (2001), Spatial and temporal characteristics of dust storms in China and its surrounding regions, 1960-1999: Relations to source area and climate, *J. Geophys. Res.*, 106, No. D10, 10,325-10,333.

Uno, I., H. Amano, S. Emori, K. Kinoshita, I. Matsui, and N. Sugimoto (2001), Trans-Pacific yellow sand transport observed in April 1998: A numerical simulation, *J. Geophys. Res.*, 106, No. D16, 18,331-18,344.

Wang, J.S., J.A. Logan, M.B. McElroy, B.N. Duncan, I.A. Megretaskaia, and R.M. Yantosca (2004), A 3-D model analysis of the slowdown and interannual variability in the methane growth rate from 1988 to 1997, *Global Biogeochem. Cycles*, 18, GB3011, doi:10.1029/2003GB002180.

Wang, K.-Y., J.A. Pyle, M.G. Sanderson, and C. Bridgeman (1999), Implementation of a convective atmospheric boundary layer scheme in a tropospheric chemistry transport model, *J. Geophys. Res.*, 104, No. D19, 23729-23745.

Wang, K.-Y., and D.E. Shallcross (2000a), A Lagrangian study of the three-dimensional transport of boundary-layer tracers in an idealised baroclinic-wave life-cycle, *J. Atmos. Chem.*, 35, 227-247.

Wang, K.-Y., and D.E. Shallcross (2000b), A modelling study of tropospheric distribution of the trace gases CFCl_3 and CH_3CCl_3 in the 1980s, *Annales Geophysicae*, 18, 972-986.

Wang, K.-Y., and D.E. Shallcross (2000c), Modelling terrestrial biogenic isoprene fluxes and its potential impact on global chemical species using a coupled LSM-CTM model, *Atmos. Environ.*, 34(18), 2909-2925.

Wang, K.-Y., D.J. Lary, and S.M. Hall (2000), Improvement of a 3-D CTM and a 4-D variational data assimilation on a vector machine CRAY J90 through a multitasking strategy, *Comput. Phys. Commun.*, 125, 142-153.

Wang, K.-Y., J.A. Pyle, and D.E. Shallcross (2001a), Formulation and evaluation of IMS, an interactive three-dimensional tropospheric chemical transport model 1. Model emission schemes and transport processes, *J. Atmos. Chem.*, 38, 195-227.

Wang, K.-Y., J.A. Pyle, D.E. Shallcross, and D.J. Lary (2001b), Formulation and evaluation of IMS, an interactive three-dimensional tropospheric chemical transport model 2. Model chemistry and comparison of modelled CH_4 , CO , and O_3 with surface measurements, *J. Atmos. Chem.*, 38, 31-71.

Wang, K.-Y., J.A. Pyle, D.E. Shallcross (2001c), and S.M. Hall, Formulation and evaluation of IMS, an interactive three-dimensional tropospheric chemical transport model 3. Comparison of modelled C2-C5 hydrocarbons with surface measurements, *J. Atmos. Chem.*, 40, 123-170.

Wang, K.-Y., D.J. Lary, D.E. Shallcross, S.M. Hall, and J.A. Pyle (2001), A review on the use of the adjoint method in four-dimensional atmospheric chemistry data assimilation, *Quart. J. Roy. Met. Soc.*, 127, 2181-2205, 2001.

Wang, K.-Y., D.E. Shallcross, and J.A. Pyle (2002), Seasonal variations and vertical movement of the tropopause in the UTLS region, *Annales Geophysicae*, 20, 871-874.

Wang, K.-Y., D.E. Shallcross, P. Hadjinicolaou, and C. Gianakopoulos (2002), An efficient chemical systems modelling approach, *Environmental Modelling & Software*, 17, 731-745.

Wang, K.-Y., Shallcross, D.E., Hadjinicolaou, P., Giannakopoulos (2004), C., Ambient vehicular pollutants in the urban area of Taipei: Comparing normal with anomalous vehicle emissions, *Water, Air, and Soil Pollution* 156, 29-55.

Wang K.-Y., P. Hadjinicolaou, G.D. Carver, D.E. Shallcross, and S. Hall (2005), Wang, K.-Y., D.E. Shallcross, S.M. Hall, Y.-H. Lo, C. Chou, and D. Chen, DOBSON: A Pentium-Based SMP Linux PC Beowulf for distributed-memory high resolution environment modelling, *Environmental Modelling & Software*, 20, 1299-1306.

Wang K.-Y., P. Hadjinicolaou, G.D. Carver, D.E. Shallcross, and S. Hall (2005), Generation of low particle numbers at the edge of the polar vortex, *Environmental Modelling & Software*, 20, 1273-1287.

Wang, K.-Y. (2005), A 9-year climatology of airstreams in East Asia and implications for the transport of pollutants and downstream impacts, *J. Geophys. Res.*, 110, D07306, doi:10.1029/2004JD005326.

Wang, K.-Y., and D.E. Shallcross (2005), Simulation of the Taiwan climate using the Hadley Centre PRECIS regional climate modelling system: The 1979-1981 results, *Terr. Atmos. Oceanic Sci.*, 16, 1017-1043.

Wang, K.-Y., and S.-A. Liao (2006), Lightning, radar reflectivity, infrared brightness temperature, and surface rainfall during the 2-4 July 2004 severe convective system over Taiwan area, *J. Geophys. Res.*, in press.

Wang, K.-Y. (2007), Long-range transport of the April 2001 dust clouds over the subtropical East Asia and the North Pacific and its impacts on ground-level air pollution : A Lagrangian simulation, *J. Geophys. Res.*, 112, D09203, doi:10.1029/2006JD007789.

Wang, Y. Q., L.R. Leung, J.L. McGregor, D.K. Lee, W.C. Wang, Y.H. Ding, and F. Kimura (2004), Regional climate modeling: Progress, challenges, and prospects, *J. Meteor. Soc. Jpn.*, 82, 1599-1628.

Wilderspin, B. (2002), Book review: Improve the effectiveness of U.S. climate modeling, *Weather*, 57, 463.

Wong S., W.-C. Wang, I. S. A. Isaksen, T. K. Berntsen, J. K. Sundet (2004), A global climate-chemistry model study of present-day tropospheric chemistry and radiative forcing from changes in tropospheric O₃ since the preindustrial period, *J. Geophys. Res.*, 109, D11309, doi:10.1029/2003JD003998.